# A Bifurcation Analysis of The Forced van der Pol Oscillator

Arun Sharma

140281167

MTHM038

2014/15

A thesis presented for the degree of

Master of Mathematics

Supervised by Prof W. Just

Department of Mathematics

Queen Mary University of London

## Abstract

In this paper we explore the dynamics of a nonlinear damped differential equation, the Forced van der Pol Oscillator. We have done this by constructing the systems bifurcation diagram as it offers a concise and qualitative way of measuring the systems dependence on certain bifurcation parameters. We go on to conclude that the system is invariant symmetric about our two subject bifurcation parameters, as well as convergent to fixed point solutions along one parameter axis and a stable limit cycle along the other parameter axis. The system is found to undergo a Saddle-node bifurcation when an eigenvalue becomes zero, as well as a Supercritical Hopf bifurcation due to a pair of complex conjugate eigenvalues. These both collectively split the bifurcation diagram into different regions. We also show that one of the two calculated Saddle-node branches is actually a global, Infinite-period bifurcation, which is due to the oscillations period increasing to infinity, creating a saddle point.


## Acknowledgements


I am deeply grateful to my supervising Professor Wolfram Just for his exceptional guidance and support throughout this thesis. I thank him for his patience and encouragement whenever my progression stalled, and accredit the completion of this paper to his outstanding teaching ability.

# 1 Introduction

Balthazar van der Pol was a pioneer in telecommunications and an electrical engineer who when building electronic circuit models of the human heart, began to study the triode oscillations he encountered in his work. To describe the periodic orbits he found, Balthazar formulated his now famous equation, the Van der Pol oscillator. The van der Pol equation is a classical example of a self oscillating system with nonlinear damping. Energy is generated at low amplitudes and dissipated at high, and typically gives birth to what's known as a limit cycle. Researching the dynamical properties these periodic solutions hold have become increasingly popular over recent years, and due to the nature of the equation, it has become fundamental in describing oscillating systems. To this date the van der Pol Oscillator has been used in several applications in diverse fields such as biology, meteorology and sociology [1, 2].

Due to its vast applications and unique characteristics, better understanding the van der Pol oscillator will shed light on the properties many of these oscillating systems hold and also the potential for new applications. Therefore this paper sets out to examine the dynamics of the system by constructing it's Bifurcation diagram.

## 1.1 Method of analysis - Bifurcation diagram

Jules Henri Poincaré originally coined the term bifurcation when describing the separating of equilibrium solutions in differential equations. His work showed that given a system of differential equations that are dependent on a certain parameter, the topological type of flow can alter as this parameter varies and several branches of equilibria can come together to form a bifurcation point. Since then many classes of flows have been identified, and because of this bifurcation diagrams have become useful tools in Mathematics for understanding how qualitative changes in flows can arise due to varying parameters. Fixed points can be created or destroyed and their stability can be altered, which can all be graphically represent on a single graph [1, 3]. Hence by constructing this diagram for the van der Pol Oscillator, one can gain a better understanding for the systems dependence on certain bifurcation parameters and represent the information in a concise, graphical manner. To do this, this paper will be looking at the Saddle-node, Hopf and Infinite-point bifurcations, as they sufficiently cover most of the systems dynamics. The mathematical program *Matlab* will be used to numerically portray any plots, the bifurcation diagram and it's dynamics, and the built-in function *ode45* will generate the phase space diagrams for the systems differential equations. But now we shall move onto the actual formula.

## 2 The Forced van der Pol Oscillator

We shall be using the following form of the system taken from [1]

$$\ddot{x} + \alpha\phi(x)\dot{x} + x = \beta p(t), \tag{1}$$

where $\phi(x)$ is even and $< 0$ for $|x| < 1$, and $\phi(x) > 0$ for $|x| > 1$. $p(t)$ is periodic for T and $\alpha, \beta$ are nonnegative parameters that are $\ll 1$. Now following [1]'s work, rewriting the equation as an autonomous system and making a $\frac{2\pi}{\omega}$ periodic transformation, the system can become

$$\dot{u} = u - \sigma v - u(v^2 + u^2) \tag{2}$$

$$\dot{v} = \sigma u + v - v(v^2 + u^2) - \gamma. \tag{3}$$

This shall be the Forced van der Pol variant that we use throughout the paper, where the 2 bifurcation parameters we shall be studying in more detail are $\sigma$ and $\gamma$.

# 3 Symmetry

We begin by exploring the symmetrical properties of the transformed Forced van der pol Oscillator (2) and (3) in order to reduce any unnecessary computations. As $\gamma$ and $\sigma$ are the bifurcation parameters to be examined, the symmetries for the system shall be subject to them alone.

By substituting $u \to -u$ and $v \to -v$ into (2) and (3), the first symmetry for the $\gamma$ parameter can be explored, leading to

$$\dot{u} = -u + \sigma v + u(v^2 + u^2) \tag{4}$$

$$\dot{v} = -\sigma u - v + v(v^2 + u^2) - \gamma. \tag{5}$$

Equation (4) now represents $-\dot{u}$ while equation (5) represents $-\dot{v}$ with a $-\gamma$. Therefore it is evident that the dynamics of $\dot{u}$ and $\dot{v}$ are invariant under the substitution $\gamma \to -\gamma$. Hence, the oscillator will resemble a system that as a whole has begun to rotate as $\gamma$ passes through 0 into $-\gamma$, yet will retain the same fundamental characteristics.

Now again using a similar analyses for negative time $t \to -t$ and $u \to -u$, the symmetry for the $\sigma$ parameter can be explored. (2) and (3) then become,

$$\dot{u} = -u - \sigma v + u(v^2 + u^2) \tag{6}$$

$$-\dot{v} = -\sigma u + v - v(v^2 + u^2) - \gamma. \tag{7}$$

By now setting $\sigma \to -\sigma$ it is evident that (6) becomes $-\dot{u}$ and (7) becomes $\dot{v}$. When $\gamma = 0$ the system will revert it's rotation and oscillate in the other direction, and as the systems flow is continuous, the same will occur for small $\pm\gamma$. Therefore (2) and (3) also share symmetries and retain their fundamental characteristics as $\sigma \to -\sigma$.

Consequently by combining both symmetries, the overall bifurcation diagram and analysis can be condensed as each quadrant of the diagram repeats itself in a symmetrical manner. Hence only a single quadrant needs to be constructed to fully understand the systems bifurcation diagram.

This conclusively means that only values of $\gamma \geqslant 0$ and $\sigma \geqslant 0$ will be considered as it will significantly simplify the calculations. We therefore move onto the initial bifurcation analysis for the system.

## 4 Special Cases

We begin by analytically solving the system for certain 'special' parameter values as this will form the basis for the global bifurcation diagram and analysis. The special cases give birth to both fixed points as well as a stable limit cycle, and are found

along the lines $\gamma = 0$ and $\sigma = 0$. However due to the systems spherically dynamics, we first impose polar coordinates to further discretize the system.
This is begun by making the substitutions $u = rcos\theta$ and $v = rsin\theta$, along with using the identity

$$u^2 + v^2 = r^2. \tag{8}$$

Differentiating the above formula with respect to time yields

$$u\dot{u} + v\dot{v} = r\dot{r}, \tag{9}$$

where we then substitute in (2) and (3) to obtain

$$\dot{r} = r - r^3 - \frac{\gamma v}{r} \tag{10}$$

or

$$\dot{r} = r - r^3 - \gamma sin\theta \tag{11}$$

This is the first of two formulas and describes the radial velocity of the system, and in order to calculate the rotational velocity $\dot{\theta}$, we make use of the second identity (12) (taken from [3]),

$$u\dot{v} - v\dot{u}. \tag{12}$$

Substituting $u = rcos\theta$ and $v = rsin\theta$ into (12) returns

$$r^2\dot{\theta}, \tag{13}$$

and we again use identity (12) but now with (2) and (3) to return

$$r^2\sigma - u\gamma. \tag{14}$$

Therefore by equating equations (13) and (14), as they are both derived from identity (12), we can use them to formulate a function where $\dot{\theta}$ is the subject,

$$\dot{\theta} = \sigma - \frac{\gamma cos(\theta)}{r}. \tag{15}$$

This is now the formula for the rational velocity of the system Forced van der pol system, and with both polar coordinate equations, we can now explore the special cases.

## 4.1 Along the line $\gamma = 0$

Before we begin this section, the reader must fully understand what is meant by a *fixed point* and it's stability, and therefore we shall summarise [3]'s example on fixed points.

Given that a one-dimensional system's flow is governed by $\dot{x} = f(x)$, the system will flow to the right when $f(x) > 0$ and to the left when $f(x) < 0$. At any point at which the flow stops we encounter what is known as a fixed point, an equilibrium solution defined by $f(x^*) = 0$, and the stability of this equilibrium point is defined by the flow at sufficiently small distances. If a system converges back to a fixed point when studying the flow on either side of an equilibrium point, we say this is a stable fixed point. Conversely, if the system diverges away, we say the fixed point is unstable. The above summary of fixed points and their stability is portrayed in Figure 1, where a black circle represents a stable and hollow represents an unstable fixed point.

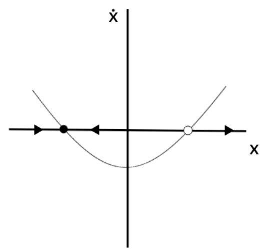


Figure 1: The vector field for the one-dimensional system, $\dot{x} = f(x)$.

Therefore with an understanding for the nature of fixed points we can move onto the first case $\gamma = 0$, where we find that the system produces a stable limit cycle and can verify this by setting $\gamma = 0$ in (11) and (15) to yield

$$h(r) = \dot{r} = r - r^3 \tag{16}$$

and

$$\theta = \sigma t + constant. \tag{17}$$

By graphically representing (16) we can show it to have a stable solution at $r = 1$, or in other words, a stable fixed point.

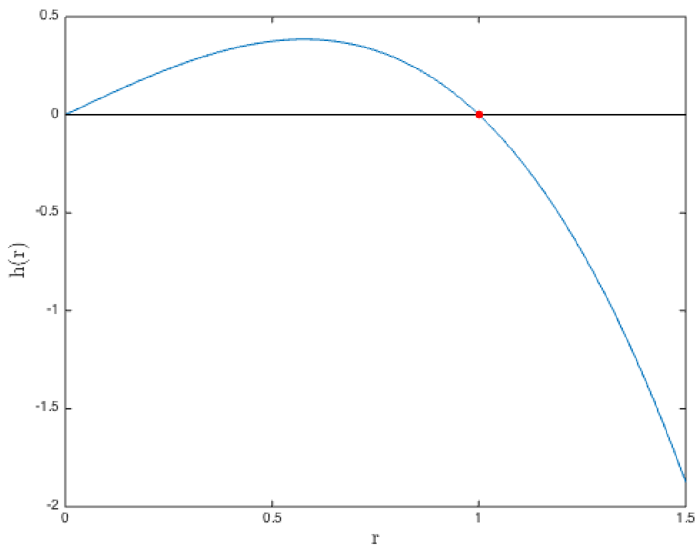


Figure 2: Plot of (16) where the red dot at $r = 1$ symbolises a stable fixed point.

This however means that as $t \to \infty$, $r(t) \to 1$, and concludes that there exists a stable limit cycle.

This emphasises that for any parameter value $\sigma$, the system will always converge into a stable, symmetrical limit cycle if $\gamma = 0$, as portrayed in Figure 3.

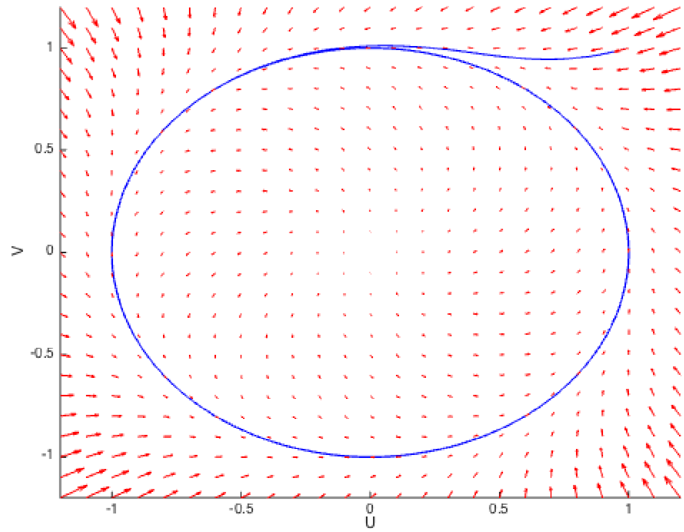


Figure 3: The Forced van der Pol system converging to a stable, symmetrical limit cycle of radius length 1, when $\gamma = 0$ and $\sigma = 0.5$

## 4.2 Along the line $\sigma = 0$

Now by evaluating both $\dot{r} = 0$ and $\dot{\theta} = 0$, the fixed point solutions along the line $\sigma = 0$ can be uncovered. Using these with (11) and (15) lead to

$$\gamma sin\theta = r - r^3 \tag{18}$$

and

$$\frac{\gamma cos(\theta)}{r} = 0, \tag{19}$$

where the solution to (19) for $\theta$ is found to be $\frac{\pi}{2}$. Subbing $\theta = \frac{\pi}{2}$ into equation (18) yields

$$\gamma = r - r^3, \tag{20}$$

where Figure 4 graphically represents the different type of fixed point solutions for $\gamma$.

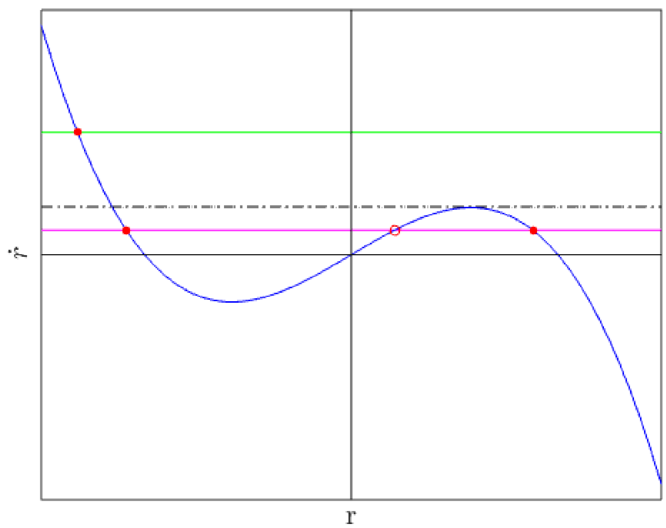


Figure 4: This figure is a graphical representation of (20) where the full horizontal lines portray solutions with 1 or 3 fixed points, and the dotted line is the boundary where the number of fixed point solutions change - there exists a saddle point on this line. In this graph a red dot represents a stable point and a red circle is unstable.

From the above figure it is clear that if $0 \leqslant \gamma < \frac{2}{3\sqrt{3}}$, there are 3 fixed points where 2 are stable and 1 is unstable, and if $\gamma > \frac{2}{3\sqrt{3}}$, there is 1 stable fixed point. Therefore, the oscillating dynamics of the system are destroyed along $\sigma = 0$, and depending on the second bifurcation parameter, will either converge to 1 or 2 stable points (Figure 5).

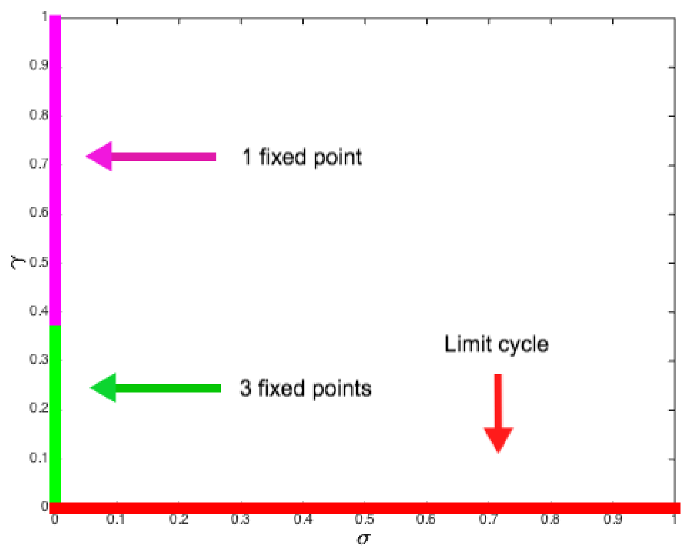


Figure 5: This graph portrays the boundary parameter conditions for the system. Along the red line there exists a stable, symmetrical limit cycle, along the green we have 3 fixed points and along the purple we have 1 fixed point.

Now that the special cases have been considered, the more elusive Saddle-node, Hopf and Global bifurcations can be explored.

# 5 Saddle-node Bifurcations

The Saddle-node bifurcation is a tool for analysing the creation or destruction of fixed points in a system, the fixed points move closer as a parameter varies and eventually collide to mutually annihilate each other. At this point the derivative of the Jacobian is 0, which occurs due to a zero eigenvalue [1, 3]. To illustrate how this works we shall be highlighting a section from [3]'s work on the first order system

$$\dot{x} = r + x^2.$$

[3] demonstrates that for varying $r$, the system undergoes a Saddle-node bifurcation where the system goes from having 2 fixed points, $x^*$, to a saddle point and then to none (Figure 6).

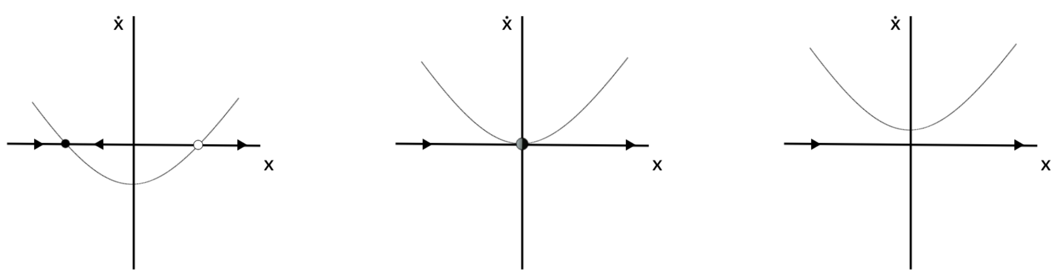


Figure 6: On the left we have $r < 0$, in the middle $r = 0$ and the right $r > 0$.

Therefore as $r \to 0^-$ the parabola pushes up, forcing the 2 fixed points to converge until they form a saddle point, a half stable point at $r = 0$ ($x^* = 0$). As $r > 0$, this point vanishes and any fixed points the system had are now destroyed. Hence we recognise that the system has successful undergone a Saddle-node bifurcation at $r = 0$. For the Forced van der pol oscillator we find that system undergoes a Saddle-node bifurcation along a given trajectory for $\sigma$ and $\gamma$. Therefore we begin by noting that we require the solutions to the system where the fixed points are mutually annihilated, $u_*$ and $v_*$, and where the system has a 0 eigenvalue leading to a determinant = 0.

### 5.1 Formulating $\mathbf{u}_*$ and $\mathbf{v}_*$

Hence, by equating (2) and (3) to 0, they can be rearranged to yield

$$0 = u_* - \sigma v_* - u_* r_*^2 \tag{21}$$

$$\gamma = \sigma u_* + v_* - v_* r_*^2, \tag{22}$$

where the fixed points version of (8), $u_*^2 + v_*^2 = r_*^2$ have been used. Now, rewriting (21) and (22) in matrix form, they can be solved for $u_*$ and $v_*$ to yield the fixed points solutions.

$$u_* = \frac{\gamma\sigma}{(1 - r_*^2)^2 + \sigma^2} \tag{23}$$

$$v_* = \frac{\gamma(1 - r_*^2)}{(1 - r_*^2)^2 + \sigma^2}. \tag{24}$$

*Please see Appendix 10.1 for calculations.*

Equations (23) and (24) now describe the systems Saddle-node points, but can be analytically used to formulate separate trajectory formulas for both $\sigma$ and $\gamma$, both in terms of just $r_*^2$.

## 5.2 Formulating $\sigma$ and $\gamma$

Again using relation (8) but now with the newly constructed (23) and (24), we find that,

$$r_*^2 = \frac{\gamma^2}{\sigma^2 + (1 - r_*^2)^2} \tag{25}$$

or

$$\gamma^2 = r_*^2(\sigma^2 + (1 - r_*^2)^2). \tag{26}$$

Now utilizing the zero eigenvalue condition allows us to set the determinant of the Jacobian equal to 0, which we must do in order to construct an equation in terms of $\sigma$. Thus

$$det \begin{bmatrix} 1 - v_*^2 - 3u_*^2 & -\sigma - 2u_* v_* \\ \sigma - 2u_* & 1 - u_*^2 - 3v_*^2 \end{bmatrix} = \begin{bmatrix} 0 \end{bmatrix}, \tag{27}$$

which can be re-arranged for $\sigma^2$ to produce

$$\sigma^2 = 4r_*^2 - 3r_*^4 - 1, \tag{28}$$

*Please see Appendix 10.2 for calculations.*

with the positive root

$$\sigma = \sqrt{4r_*^2 - 3r_*^4 - 1}. \tag{29}$$

Therefore the above formula is the Saddle-node bifurcation trajectory for our first parameter $\sigma$, and is only in terms of $r_*^2$, as earlier stated. Now subbing (28) into (26) yields the formula for the second parameter, $\gamma^2$, again only in terms of $r_*^2$,

$$\gamma^2 = 2r_*^4(1 - r_*^2), \tag{30}$$

with positive root

$$\gamma = \sqrt{2r_*^4(1 - r_*^2)}. \tag{31}$$

As (29) is strictly $> 0$ when $\frac{1}{\sqrt{3}} < r_* < 1$, we only consider these values of $r_*$ for $\sigma$, and as (31) is strictly $> 0$ for $0 < r_* < 1$, we again only consider these values of $r_*$ for $\gamma$ (we have neglected negative $r_*$ values as $r_*$ is by definition positive). Therefore plotting (29) against (31) both from $0 < r_* < 1$, while neglecting the imaginary values for (29), results in Figure 7.

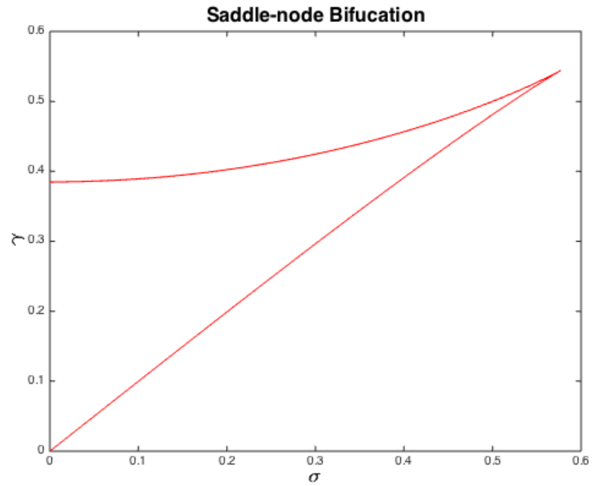


Figure 7: The Forced van der pol Saddle-node bifurcation plot. The trajectories mark the boundaries where the systems oscillating dynamics fundamentally change.

Figure 7 demonstrates the destructive nature of the bifurcation parameters and splits the quadrant into different sections where fixed points are either known to exist or not. Unlike with the special cases, Figure 7 is the first real analysis of the relationship between both parameters when they are both non-zero, and their affect on the systems fixed points. However Figure 8 expresses how damaging the creation of fixed points can be to a limit cycle's flow, and how this can be achieved with minor parameters changes.

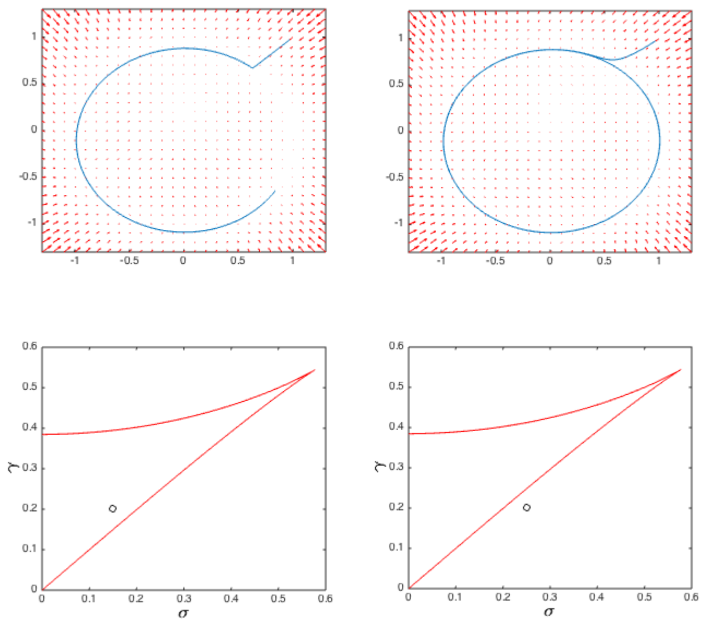


Figure 8: Here we have the Forced van der pol system when $\gamma = 0.2$, as well as $\sigma = 0.15$ and $\sigma = 0.25$ from left to right respectively. In the chapter on Global bifurcations we see that the Saddle-node branch examined in this plot is actually an Infinite-period bifurcation, which occurs along a saddle-node trajectory.

We now move onto the next section that explores the creation of limit cycles from stable fixed points, or vice versa, and what is known as a Hopf bifurcation.

# 6 Hopf Bifurcation

The Hopf bifurcation is another useful tool for understanding the dynamics of differential equations, and is able to quantify the conditions needed for a stable fixed

point loose stability. Given a two-dimensional system where both eigenvalues have Re $\lambda < 0$, the system will converge to a stable fixed point. However if a parameter varies and forces at least one of the eigenvalues to obtain a Re $\lambda > 0$ or both to become complex conjugates $(+iw, -iw)$, the fixed point will lost stability and undergo a Hopf bifurcation.
Obtaining complex conjugate eigenvalues will force the system into a limit cycle; although the reverse is also possible, a limit cycle can be reverted back into a stable fixed point by obtaining two eigenvalues with Re $\lambda < 0$ [1, 3].

There are 2 possible types of Hopf bifurcations, a Supercritical or Subcritical. If a *decay* parameter moves past a critical threshold to become a *growth*, the equilibrium state will loose stability and the system will undergone a Supercritical Hopf bifurcation (Figure 9).

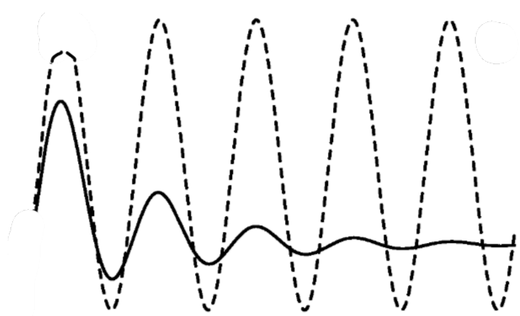

Figure 9: An illustration of the amplitude over time of a system that has undergone a Supercritical Hopf bifurcation. The full line is the parameter value that falls below the threshold, *decay*, and the dotted line falls above the bifurcation threshold, *growth*.

If the trajectory jumps to an attractor in the form of a fixed point, limit cycle or infinity after the system bifurcates, the system has undergone a Subcritical Hopf bifurcation [3].

Nevertheless we can analytically compute the conditions for the Hopf bifurcation for the van der Pol system by recalling that it's eigenvalues must be complex conjugate. This of course yields a $Determinant(Jacobian) > 0$ and a $Trace(Jacobian) = 0$. Therefore by using these conditions, an equation describing the trajectory for the Hopf bifurcation can be formulated in terms of $\sigma^2$ and $\gamma^2$, similarly to Saddle-node section.

## 6.1 Radial length

We begin by calculating the Hopf bifurcation point using the fixed point solutions for (2) and (3), again like the saddle-node section. However we then utilise the $Trace$ condition to conclude that

$$r_*^2 = \frac{1}{2} \tag{32}$$

is the radial length the Hopf bifurcation occurs at. We will use this solution in the next subsection to solve our formulas for $\sigma^2$ and $\gamma^2$.

## 6.2 Formulating $\sigma$ and $\gamma$

By now evaluating the $Determinant(Jacobian) > 0$ condition yields the relation

$$\sigma^2 > 4r_*^2 - 3r_*^4 - 1, \tag{33}$$

*Please see Appendix 10.2 for calculations of a similar type.*

which is a re-written version of (28). Furthermore by taking (32) and subbing it into (26), we produce the following hyperbola

$$\gamma^2 = \frac{1}{2}\sigma^2 + \frac{1}{8}, \tag{34}$$

which is portrayed in Figure 10.

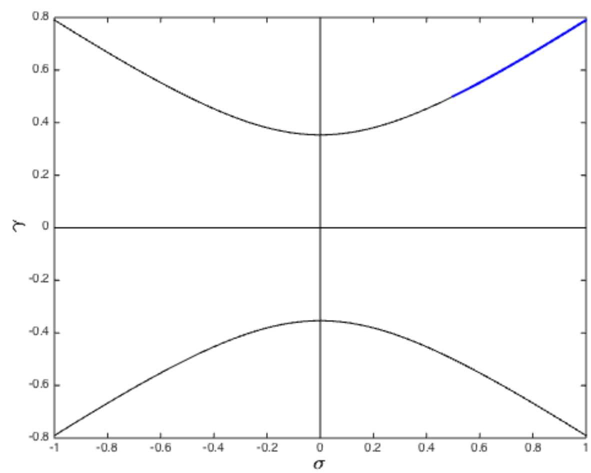


Figure 10: This graph is for the entire hyperbola, equation (34), stretching over the 4 bifurcation quadrants.

The above plot, Figure 10, portrays the entire hyperbola plane, however we only require the North-Eastern quadrant due to the earlier mentioned symmetries.

Finally we use relation (32) with (33) and substitute this value into (34) to return the bifurcation conditions for the hyperbola. These are,

$$\sigma > \frac{1}{2} \tag{35}$$

and

$$\gamma > \frac{1}{2} \tag{36}$$

Utilising all of the given information we can conclude that the Hopf bifurcation begins at $(\sigma, \gamma) = (\frac{1}{2}, \frac{1}{2})$ and continues onwards for growing $\sigma$ and $\gamma$. This is represented in Figure 10 as the blue curve in the north-eastern quadrant.

By graphically representing both the Saddle-node and Hopf bifurcation together we obtain Figure 11 and 12.

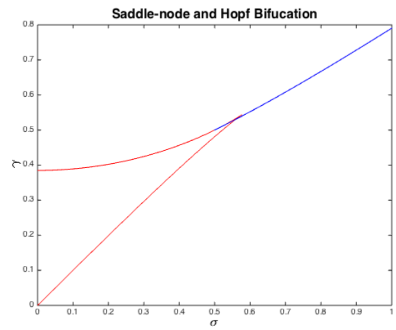


Figure 11: This graph represents both the Saddle-node and Hopf bifurcation. A red line portrays the Saddle-node trajectory while the blue line is the Hopf trajectory

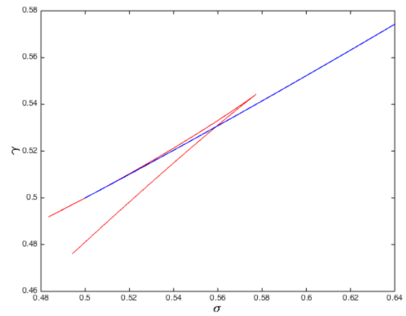


Figure 12: Zoomed portrait of Figure 11, showing how the Hopf bifurcation begins at $(\sigma, \gamma) = (\frac{1}{2}, \frac{1}{2})$ and crosses through the Saddle-node trajectory.

With the newly found information we can numerically plot the systems behaviour and actually see the Hopf bifurcation take place. Additionally as [3] suggests, we can also distinguish what type of Hopf bifurcation occurs.

By studying Figure 13 it is clear that the system has undergone a Supercritical Hopf bifurcation. This is because the systems amplitude quickly grows into a stable oscillation as $\sigma$ passes beyond the Hopf bifurcation threshold, and does not jump to any distance attractors.

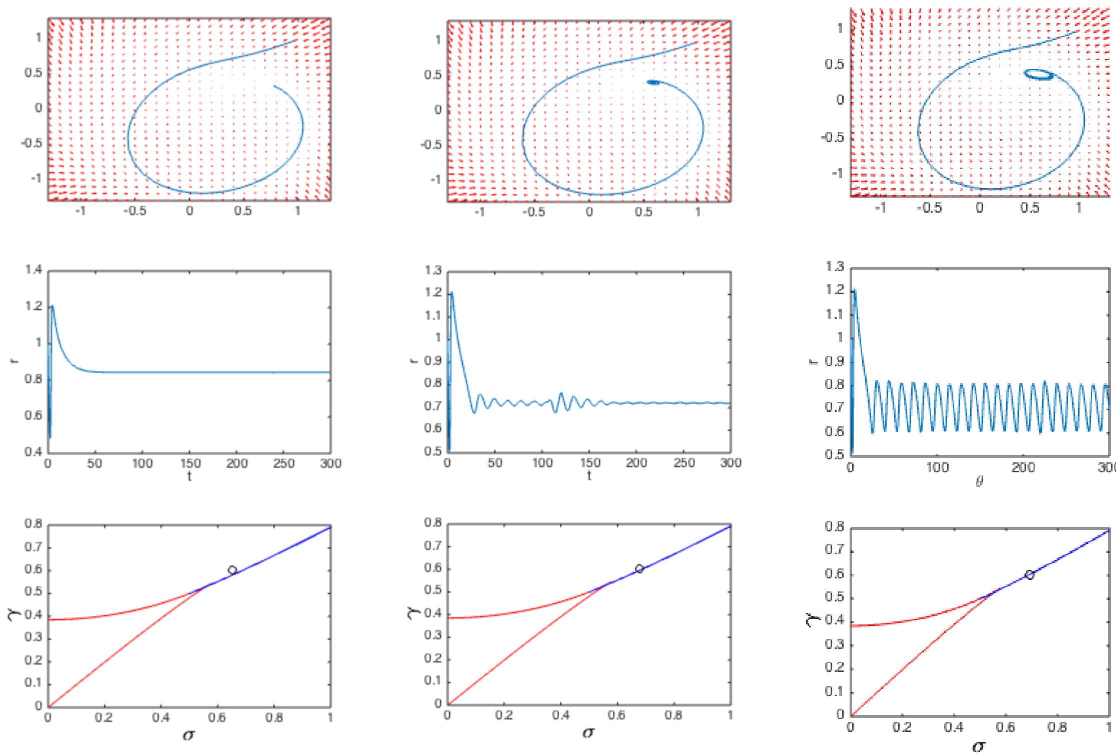


Figure 13: These 3 plots portray how the Forced van der Pol systems behaves as we cross the Hopf bifurcation line with $\gamma = 0.6$ and an alternating $\sigma$. On the left $\sigma = 0.65$, in the middle $\sigma = 0.68$ and on the right $\sigma = 0.69$. Nevertheless despite somewhat resembling a 'perfect' 'circle, in reality the system converges to a deformed circle.

Furthermore as the right hand set of plots in Figure 13 highlights, the system has successfully formed a limit cycle. From our Special cases analysis we deduced that a limit cycle must also exist on the $\sigma$ boundary axis, therefore no further bifurcations can occur in-between. This means that the only qualitative change we exhibit is between a single fixed point and a single limit cycle as the system crosses the Hopf boundary line right down to the axis boundary, respectively. This once again confirms a Supercritical Hopf bifurcation.

We now explore the final type of bifurcation, a global bifurcation that can create or destroy limit cycles throughout large regions of the phase space as opposed to a fixed point segment.

# 7 Global Bifurcations

## 7.1 Infinite-period Bifurcation

The Infinite-period bifurcation is a method that quantifies the conditions needed to destroy or create a limit cycles with the use of fixed points in a system. They can arise when the speed of an oscillating system slows down as a parameter reaches a critical threshold. The oscillation period lengthens and diverges to infinity as the parameter reaches the critical value; a fixed point appears in result and we say that the system has undergone an Infinite-period bifurcation. Beyond the critical parameter value, 2 fixed points appear and the system becomes phase locked [3]. This can be a global phenomenon and is why it's important to consider, hence we use [3]'s example as an illustration.

Given the system

$$\dot{r} = r(1 - r^2)$$

$$\dot{\theta} = \mu - sin\theta$$

where $\mu \geqslant 0$, it's concluded that the system approaches the unit circle while rotating counterclockwise if $\mu > 1$. However as $\mu$ decreases through 1 the oscillations period increases, eventually becoming infinite as $\mu = 1$. Thus a single fixed point is created, the limit cycle is destroyed, and the system has undergone a Infinite-period bifurcation. If $\mu < 1$ the single fixed point will split into 2 fixed points, and an example of the starting and ending states are illustrated in Figure 14.

Figure 14: On the left we have a stable limit cycle with an unstable fixed point, $\mu > 1$, and on the right we have a phase locked limit cycle with 3 fixed points, $\mu < 1$.

Hence we now use the van der Pol system in polar coordinate form and more importantly, equation (15), as this equation describes the orbital velocity of the system.

When examining (15) we find that the system rotates counterclockwise globally when $\dot{\theta} > 0$ or $\sigma > \frac{\gamma}{r}$ for all $r \in (0, \infty)$. As $\sigma$ decreases through $\sigma = \frac{\gamma cos\theta}{r}$, the rotation changes direction and 2 fixed points are born, an unstable point and a stable point. Therefore a bottle neck is created around the saddle point $\theta = 0$, where the oscillations period increases severely as $\sigma \to \frac{\gamma}{r}^+$ (Figure 15). This Saddle point is also where the Infinite-period bifurcation takes place, and the 3 possible solution states for (15) are all portrayed in Figure 16.

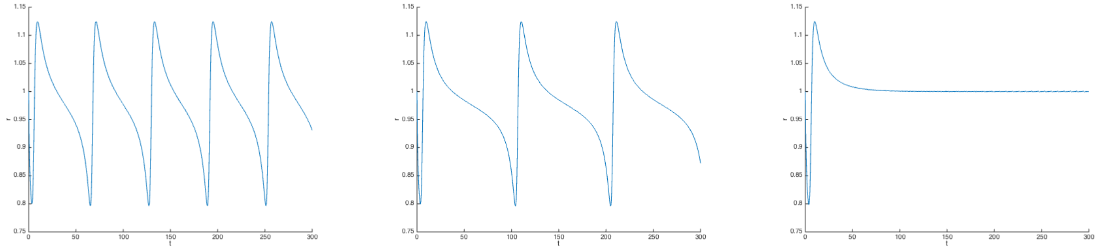

Figure 15: This represents the diverging length of oscillations for the van der Pol system as $\sigma$ crosses the critical value, $\sigma = \frac{\gamma}{r}$. In the final plot we can see that the oscillations period has diverged to infinity.

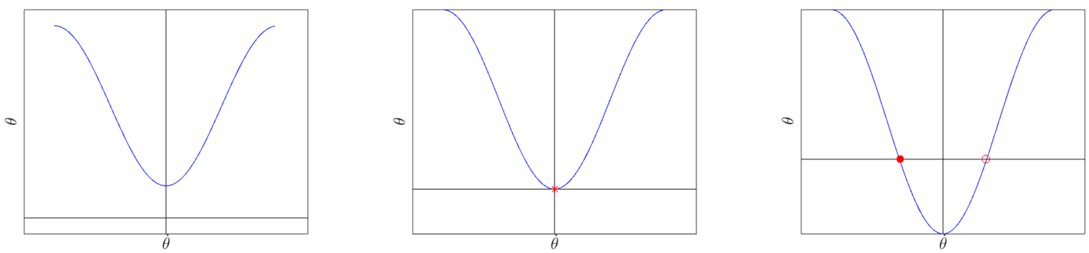

Figure 16: These 3 plots represent the different solutions for (15). From left to right we have no fixed point solutions, $\sigma > \frac{\gamma}{r}$, then a Saddle-point when $\sigma = \frac{\gamma}{r}$, marked by a red star, and finally 2 fixed points when $\sigma < \frac{\gamma}{r}$, the red dot corresponds to a stable point while a circle corresponds to an unstable point.

From this we can conclude that the Infinite-point bifurcation occurs along one of the two Saddle-node lines calculated in section 5, which was previously mentioned and represented in section 5.2 Figure 8.

Now with all of the previously calculated bifurcations, a concluding topological argument can be deduced to examine how the system behaves in the different regions of the bifurcation diagram.

# 8 Topological Analysis

In the section on Special cases we established that there exists a stable limit cycle along the axis line $\gamma = 0$ for $\sigma \to \infty$, as well as that the Hopf bifurcation line above $\gamma = 0$ (please see Figure 11) represents the destruction or creation of a limit cycle. Therefore we conclude that a limit cycle must exist in-between both boundaries (Region B Figure 17) as the system cannot exhibit discontinuous jumps when moving off the $\gamma = 0$ boundary into Region B Figure 17. Because of this we additionally find that parameter space above the Hopf bifurcation line and upper Saddle-node branch, represent a region of stable fixed points where the system has ceased to oscillate (Region A Figure 17). As an additional piece of confirmation, we find that Figure 13 agrees with the above analysis.

Furthermore, in the section on Global bifurcations it was established that an Infinite-period bifurcation occurs on a stable limit cycle at a Saddle-node point. Therefore this bifurcation must emerge from the bottom of the two Saddle-node branches, as we know that a limit cycle exists below this line (Black branch Figure 17). Therefore as the system transitions from Region B up past the lower Saddle-node branch, an Infinite-period bifurcation takes place and the system becomes phase locked. Now consider the green axial line in Figure 17 that has 3 fixed points, and the Infinite-period bifurcation branch. The area in between (Region C Figure 17) must contain 3 fixed points, 2 of which are created from the Infinite-period bifurcation and 1 from a negative radial length. For an illustration of where a negative radial length can arise from, please look at the green solution line in Figure 4.

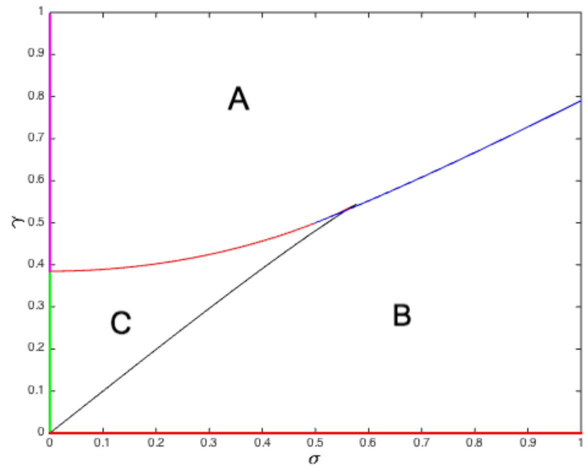


Figure 17: This is the final bifurcation diagram for the Forced van der Pol oscillator. The different colours represent the different solutions that the system can hold and that this paper has covered. While regions A, B and C represent areas of fixed points and limit cycles respectively.

# 9 Conclusion

We conclude that the Forced van der Pol system is invariant under the transformations imposed by negative $\sigma$ and $\gamma$ values, which lead to simplifying symmetries for the bifurcation diagram. The Special Cases analysis in section 4 established that for $\gamma = 0$, there exists a stable limit cycle for all $\sigma > 0$, and that when $\sigma = 0$, the system either has 3 fixed points ($\gamma < \frac{2}{3\sqrt{3}}$, green axis line Figure 17) or 1 fixed point ($\gamma > \frac{2}{3\sqrt{3}}$, purple axis line Figure 17). The Saddle-node bifurcation followed and dissected the graph into 2 regions, expressing branches where fixed points emerge on limit cycles to phase lock them. Next came the Hopf bifurcation, which begun at $(\sigma, \gamma) = (\frac{1}{2}, \frac{1}{2})$ and increased along the cut-off trajectory of a hyperbola to distinguish regions where limit cycles loose stability and turn into fixed points, or vice versa. Finally came the Infinite-period global bifurcation that was found to occur along the lower of the two Saddle-node branches, a point where the oscillations period diverges to infinity to create a saddle point. From this it was established that stable limit cycles exist underneath the Infinite-period and Hopf bifurcation trajectories, and 3 fixed points reside inside the Infinite-period and Saddle-node cusp. Lastly, above the Saddle-node and Hopf branch the system ceases to oscillate and converges to a stable fixed point.

# References

[1] Guckenheimer, J, Holmes, P. *Nonlinear Oscillations, Dynamical Systems, and Bifurcations of Vector Fields.* Applied Mathematical Sciences **42**. Springer-Verlag, New York, 1983.

[2] Tsatsos, M. *Theoretical and Numerical Study of the Van der Pol equation*. Aristotle University of Thessaloniki, Department of Physics, Mechanics. July 2006.

[3] Strogatz, S. *Nonlinear Dynamics and Chaos with Applications to Physics, Biology, Chemistry and Eingineering*. Studies in Nonlinearity, $\mathbf{1}^{st}$ edition. Westview Press, United States of America, December 2000.

# 10 Appendix

## 10.1 Appendix A

We firstly begin with

$$\begin{bmatrix} 0 \\ \gamma \end{bmatrix} = \begin{bmatrix} u_* - u_* r_*^2 - \sigma v_* \\ v_* - v_* r_*^2 + \sigma u_* \end{bmatrix}$$

which can be rewritten as,

$$\begin{bmatrix} 0 \\ \gamma \end{bmatrix} = \begin{bmatrix} 1 - r_*^2 & -\sigma \\ \sigma & 1 - r_*^2 \end{bmatrix} \begin{bmatrix} u_* \\ v_* \end{bmatrix}$$

This can now be inverted to produce,

$$\begin{bmatrix} u_* \\ v_* \end{bmatrix} = \begin{bmatrix} \frac{1-r_*^2}{(1-r_*^2)^2+\sigma^2} & \frac{\sigma}{(1-r_*^2)^2+\sigma^2} \\ \frac{-\sigma}{(1-r_*^2)^2+\sigma^2} & \frac{1-r_*^2}{(1-r_*^2)^2+\sigma^2} \end{bmatrix} \begin{bmatrix} 0 \\ \gamma \end{bmatrix}$$

and thus,

$$u_* = \frac{\gamma\sigma}{(1 - r_*^2)^2 + \sigma^2}$$

$$v_* = \frac{\gamma(1 - r_*^2)}{(1 - r_*^2)^2 + \sigma^2}.$$

## 10.2 Appendix B

Beginning with (27)

$$det \begin{bmatrix} 1 - v_*^2 - 3u_*^2 & -\sigma - 2u_*v_* \\ \sigma - 2u_* & 1 - u_*^2 - 3v_*^2 \end{bmatrix} = \begin{bmatrix} 0 \end{bmatrix},$$

we evaluate the first step of the determinate to yield

$$(1 - v_*^2 - 3u_*^2)(1 - u_*^2 - 3v_*^2) + (\sigma + 2u_*v_*)(\sigma - 2u_*v_*) = 0,$$

and then simplify it to

$$1 - 4(u_*^2 + v_*^2) + 3(u_*^4 + v_*^4) + 6u_*^2v_*^2 + \sigma^2 = 0.$$

Now by making use of the quadratic relation

$$(u_*^2 + v_*^2)^2 = v_*^4 + u_*^4 + 2u_*^2v_*^2,$$

we can re-write the above equation as

$$1 - 4r_*^2 + 3r_*^4 + \sigma^2 = 0,$$

and then

$$\sigma^2 = 4r_*^2 - 3r_*^4 - 1.$$